G Model
JALCOM-21598; No. of Pages 5

ARTICLE IN PRESS

Journal of Alloys and Compounds xxx (2010) xxx–xxx

Contents lists available at ScienceDirect

Journal of Alloys and Compounds

journal homepage: www.elsevier.com/locate/jallcom

Effect of post-CVD thermal treatments on crystallographic orientation, microstructure, mechanical and optical properties of ZnS ceramics

P. Biswas, R. Senthil Kumar, P. Ramavath, V. Mahendar, G.V.N. Rao, U.S. Hareesh, R. Johnson *

International Advanced Research Centre for Powder Metallurgy and New Materials, Hyderabad 500005, India

ARTICLE INFO

Article history:
Received 14 October 2009
Received in revised form 22 January 2010
Accepted 22 January 2010
Available online xxx

Keywords:
Ceramics
Vapor deposition
Optical properties
X-ray diffraction
Microstructure

ABSTRACT

Chemical vapor deposited (CVD) zinc sulphide samples were subjected to hot isostatic pressing (HIP) and heat treatment under pressureless (HT) sintering conditions in argon. The effects of temperature and pressure on the crystallographic orientation, microstructure, optical and mechanical properties were studied. The removal of Zn–H absorption band present in CVD ZnS can be effected by temperature increase alone as observed for CVD + HT samples. However, a significant decrease in transmission was observed in mid IR region and is attributed to the creation of residual porosity during this process. During HIPing, on simultaneous application of temperature and pressure, the Zn–H band together with the residual porosity generated during the removal of Zn–H was also eliminated. This resulted in an increase of transmission in the mid wave IR as well as in the visible spectral region due to the considerable reduction in scatter points. A substantial increase in grain size along with a highly preferred orientation along the (1 1 1) crystallographic plane was observed as evidenced by the increase in the transverse I ratio after HIP as well as heat treatment under pressureless (HT) conditions. A decrease in the mechanical properties of the samples was also observed.

1. Introduction

Zinc sulphide, a wide gap semiconductor ceramic, is a material of significant potential utilized for a variety of applications like electroluminescent devices [1–3], flat panel displays [4,5], thin film photovoltaic cells [6], photocatalysis [7] and infrared windows [8–10]. In recent years, there has been a great deal of interest in the fabrication of thin films of zinc sulphide by techniques like chemical bath deposition [11,12], RF sputtering [13], plasma assisted MOCVD [14] and dip coating [15]. Chemical vapor deposition (CVD) being a gas phase reaction provides important advantages over other methods of materials processing in view of the ease of controlling accurately the stoichiometry and purity of the product [16–18]. Moreover, the technique is quite attractive when the product demands high physical and chemical perfection with near net shaping capability. Polycrystalline zinc sulphide (ZnS) is widely used for infrared optical engineering applications by virtue of its inherent IR transparency in the spectral band width of 3–10 μm [19–21]. Deposition of complex and large area self-standing monolithic structures by CVD is a low cost technique successfully achieved through the chemical reaction of zinc vapor with hydrogen sulphide gas at elevated temperatures and low pressures [22–33]. During CVD, ZnS grains grow anisotropically and grains parallel to the substrate surface grow more rapidly by the normal mechanism leading to the development of columnar microstructure [24,25]. This material exhibits considerable scatter, especially in the visible region of the spectral band. Studies have shown that hot isostatic pressing (HIP) results in changes in orientation of grains, size of the grains and removal of residual porosity [20,24]. Additionally, the undesired zinc hydride (Zn–H) phase commonly observed in CVD ZnS can also be removed by HIPing resulting in significant increase in transmission in the visible region.

In the present study an attempt has been made to elucidate the effect of HIPing and thermal treatment under pressureless conditions on the physical, microstructural, mechanical and optical properties of CVD ZnS. X-ray diffraction and scanning electron microscopy were employed to observe the effects on crystallographic orientation and microstructure, respectively. Correlation of results with transmission properties was also attempted.

2. Experimental details

Monolithic ZnS has been grown by the CVD reaction between zinc and hydrogen sulphide at elevated temperatures of 650–750 °C and low pressures of around 50 mbar. The zinc to H_2S molar ratio was adjusted close to 1.0 and the deposition rate of 80–100 μm/h was achieved by controlling the reactant fluxes. The samples were grown on graphite substrates in the form of flat plates of dimensions 50 mm × 50 mm × 5–6 mm thickness and were machined to the specimens of 20 mm × 20 mm × 5 mm thickness.

* Corresponding author. Tel.: +91 40 2443169; fax: +91 40 24442699.
E-mail address: royjohnson@arci.res.in (R. Johnson).

0925-8388/$ – see front matter © 2010 Published by Elsevier B.V.
doi:10.1016/j.jallcom.2010.01.120

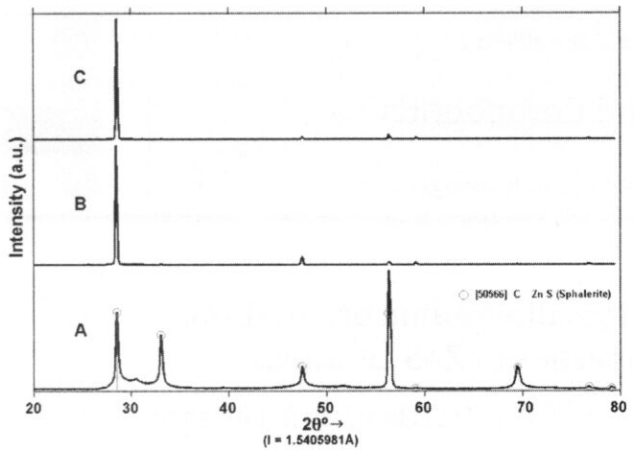

Fig. 1. XRD pattern recorded for ZnS perpendicular to the coating. (A) CVD, (B) CVD + HIP and (C) CVD + HT.

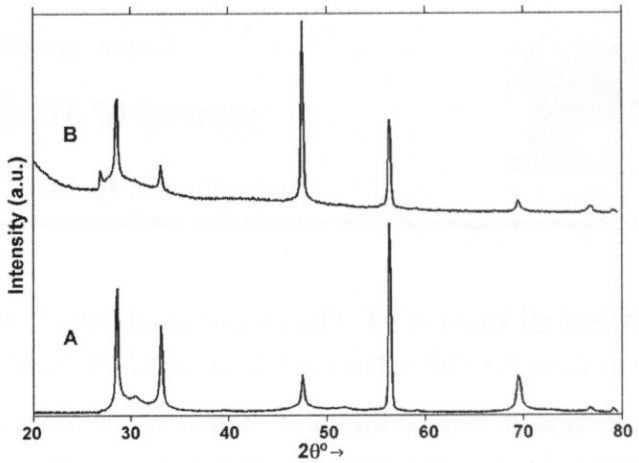

Fig. 2. XRD pattern recorded for CVD. (A) Perpendicular to direction of coating and (B) parallel to direction of coating.

The CVD specimens were hot isostatically pressed at 950 °C at 135 MPa under argon for the duration of 2 h. Alternatively, the CVD specimens were also heat treated at 950 °C under pressureless conditions in flowing argon. All samples were optically polished using standard ceramographic procedures. The CVD, CVD + HIP and CVD + heat treated samples were subjected to density measurements using helium pycnometric technique (AccuPyc 1330, Micromeritics, USA). X-ray diffraction studies (D8 Advanced, Bruker, Germany) were carried out using Cu Kα radiation, for phase analysis and crystallographic orientations. X-ray diffraction patterns were recorded parallel and perpendicular to the coating direction and the transverse I ratios were calculated using the equation $I_{(111)}/(I_{(111)} + I_{(220)})$ where $I_{(111)}$ and $I_{(220)}$ are the net area of the peaks corresponding to reflections from (1 1 1) and (2 2 0) planes.

The samples were resin mounted and polished using standard metallographic polishing procedures and were subjected to microstructural characterization by SEM (Hitachi 2400, Japan) after chemical etching for CVD samples and thermal etching at 900 °C for CVD + HIP and CVD + HT samples. The samples were also subjected to mechanical testing such as Knoop hardness (Leica, Germany) and three point bending strength measurements (Instron, UK). Transmission measurements were also carried out on samples of parallel and perpendicular orientation to the direction of deposition using FTIR (Spectrum GX, PerkinElmer, Singapore) and UV–visible (Lambda PerkinElmer, Singapore) spectroscopic techniques.

3. Results and discussion

All samples on XRD analysis have shown sphalerite phase except in case of CVD cross-section which show the evidence of (1 0 0) reflection at 2θ (26.93°) corresponding to hexagonal wurtzite phase in traces. XRD pattern of ZnS CVD, CVD + HIP and CVD + HT samples recorded on the surface that is perpendicular to the direction of deposition is shown in Fig. 1A–C, respectively. It is evident from the XRD patterns that CVD ZnS (Fig. 1A) is isotropic in comparison to the CVD + HIP and CVD + HT samples (Fig. 1B and C). In the case of CVD + HIP and CVD + HT samples all diffraction peaks disappeared or minimized except the (1 1 1) diffraction peaks where an increase in intensity was observed indicating anisotropy. The extent of anisotropy is further evident from transverse I ratio values of 0.6489 for CVD ZnS in comparison to 0.9172 and 0.9434 for CVD + HIP and CVD + HT samples, respectively (Table 1). XRD studies also confirmed that the loss of isotropy is imparted by the exposure to temperature rather than the pressure.

Table 1
Transverse I ratio calculated from XRD data.

Sample	Transverse I ratio	
	Perpendicular	Parallel
CVD	0.6489	0.3724
CVD + HIP	0.9172	0.5662
CVD + HT	0.9434	0.5574

Fig. 2A and B, Fig. 3A and B and Fig. 4A and B show the XRD pattern of the surface (perpendicular to the direction of coating) and cross-section (parallel to the direction of coating) for CVD, CVD + HIP and CVD + HT samples, respectively. A transverse I ratio of 0 6489 for CVD surface, in comparison to a value of 0.3724 for CVD cross-section is indicative of a preferred orientation of crystals perpendicular to the direction of coating. A similar trend is observed even after CVD + HIPing and CVD + HT. A transverse I ratio of 0.9172 and 0.9434 for HIP surface and HT surface in comparison to the values of 0.56621 and 0.5574 for HIP cross-section and HT cross-section, respectively indicated highly preferred orientation perpendicular to the direction of coating. The preferential orientation effect is more in case of HIPed and heat treated samples as inferred from the higher transverse I ratio difference of 0.3509 and 0.3860 compared to 0.2765 for CVD sample.

Fig. 5(A–C) shows the microstructure of the CVD ZnS, CVD + HIP and CVD + HT samples. The microstructure of CVD ZnS sample reveals a linear array of columnar grain structure oriented parallel to the direction of coating with maximum grain size distribution in the range of 5–10 μm. In addition, it is also observed that there are lamellar types of structures within the grain with elongated layers along the grain boundaries. Finer pores due to the plausible adsorption of hydrogen produced as a result of H_2S decomposition during the CVD reaction are also observed [20]. Most significant

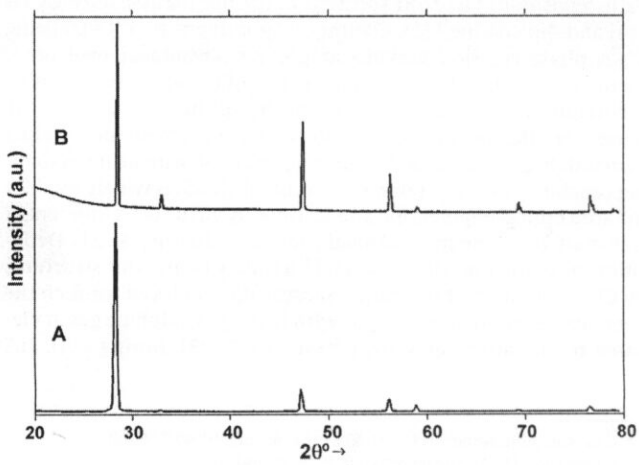

Fig. 3. XRD pattern recorded for CVD + HIP ZnS. (A) Perpendicular to direction of coating and (B) parallel to direction of coating.

Please cite this article in press as: P. Biswas, et al., J. Alloys Compd. (2010), doi:10.1016/j.jallcom.2010.01.120

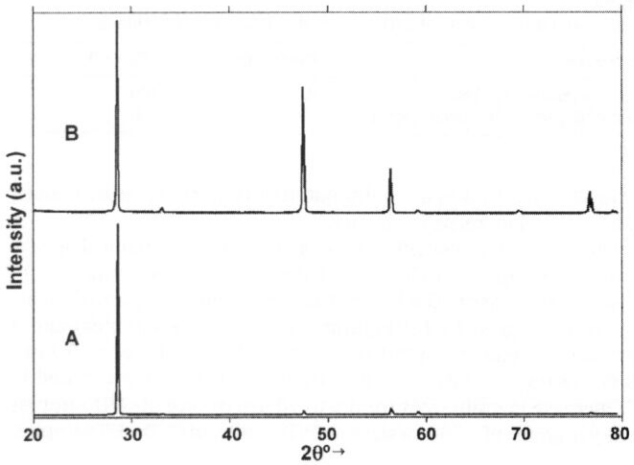

Fig. 4. XRD pattern recorded for CVD + HT ZnS (A) Perpendicular to direction of coating and (B) parallel to direction of coating.

manifestation of HIPing and heat treatment under pressureless condition on microstructure of the samples is the grain growth induced on the material leading to a substantial increase in the grain sizes (Fig. 5B). In the case of HIPing larger grains in the range of 50–100 μm with increased twin fractions were observed. Further, ZnS recrystallization also results in disappearance of conventional grain boundaries and lamellar structures from the microstructures in both the cases of HIPing and heat treatment (Fig. 5C). The microstructure of CVD + HT ZnS samples exhibited a fine distribution of residual pores and can be attributed to the decomposition of Zn–H during thermal treatment.

Fig. 6 presents the IR transmission in the spectral band of 3–10 μm for CVD, CVD + HIP and CVD + heat treated ZnS samples. The strong absorption band at 6.2 μm, typical of CVD ZnS, appeared due to the presence of zinc hydride (Zn–H) contamination formed as a result of the reaction between zinc vapor and hydrogen (by product of the CVD reaction). The average transmission is greater than 70% in the 7–10 μm region and was lowered to around 60% in the lower regions of 3–6 μm. The samples after heat treatment under pressureless conditions were free of the absorption band at 6.2 μm with a color change from yellow to white. The IR transmission reduced drastically in the region of 3–6 μm while a marginal reduction was observed in 7–10 μm region. The CVD + HIPed samples indicated a clear improvement in the transmission in 3–10 μm region and is uniformly >70%.

There are basically two reasons which may be responsible for the scattering observed at 3–6 μm regions for CVD and CVD + heat treated samples. The microporosity generated due to the adsorption of hydrogen produced during the decomposition of H_2S in CVD reactor could be a major cause of scatter and reduced transmission in 3–6 μm region for CVD samples. A closer look at the XRD patterns in Fig. 7 recorded on CVD samples perpendicular to the direction of deposition show the evidence of (1 0 0) reflection at 2θ value of 26.931° corresponding to hexagonal wurtzite phase which may also contribute to lowering of transmissions in 3–6 μm. Under pressureless heat treatment conditions, though the wurtzite phase is eliminated, the elimination of Zn–H can lead to the creation of very fine pores as is evident from the microstructure depicted in Fig. 5B. These pores in combination with the microporosity existed with CVD samples resulted in enhanced scattering leading to reduction of transmission values.

The simultaneous application of temperature and pressure through HIPing resulted in removal of microporosity as indicated by the microstructure in Fig. 5B. A homogenization to sphalerite cubic phase was also observed as supplemented by XRD patterns

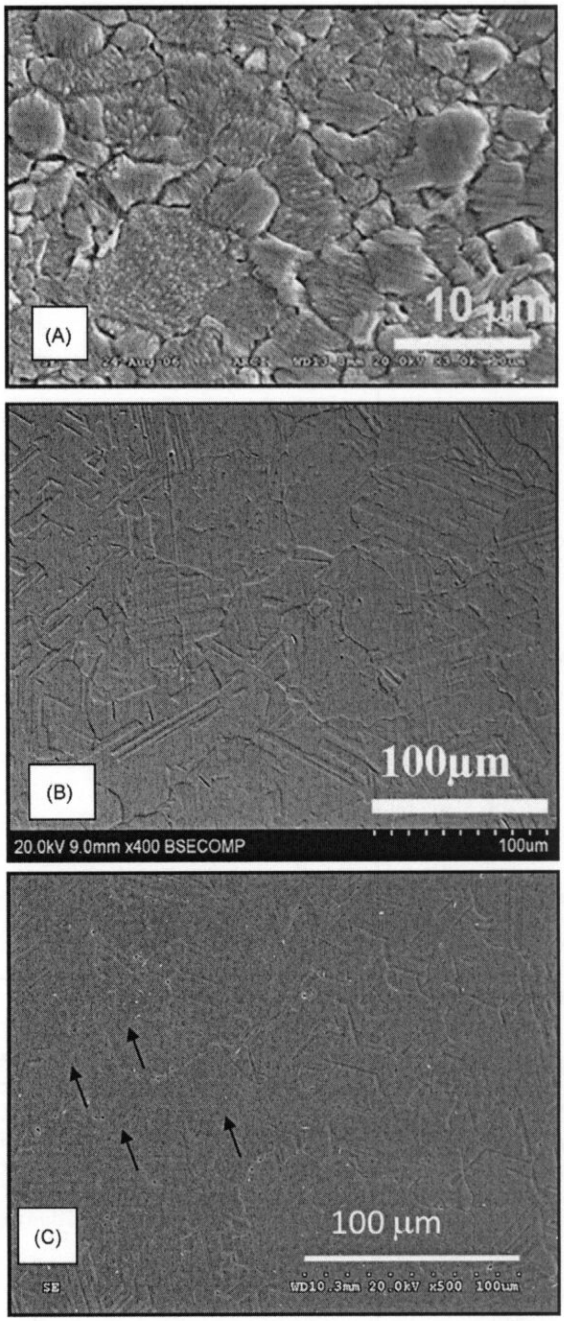

Fig. 5. Microstructure recorded for (A) CVD ZnS, (B) CVD + HIP and (C) CVD + HT.

in Fig. 7. The FTIR pattern also indicated enhanced transmission in 3–6 μm in case of HIPed samples (Fig. 6). This can also be attributed to the growth of grains from 10 μm to around 50 μm for CVD + HIP ZnS as a result of HIPing leading to reduced grain boundary scattering. The visible transmission pattern provided in Fig. 8 indicated an increased transmission in the visible region to around 68%. The transmission in the visible region was found to be less than 1% in case of CVD and CVD + heat treated samples. Though the grain growth and homogenization to sphalerite cubic phase was observed with CVD + heat treated samples, microporosity is the major cause of scatter and low transmission value.

Helium pycnometric measurements on CVD samples have exhibited a density value of 4.0850 g/cm^3 in comparison to a

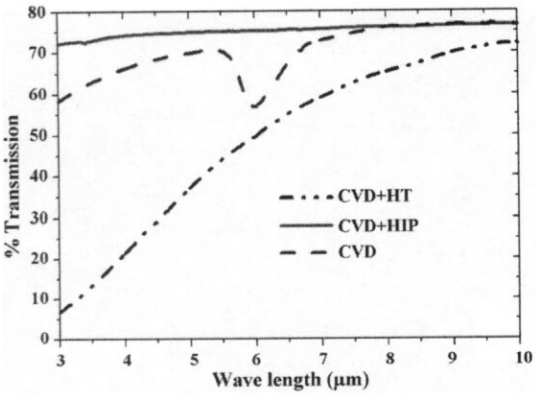

Fig. 6. FTIR transmission patterns recorded for CVD, CVD + heat treated, CVD + HIP samples.

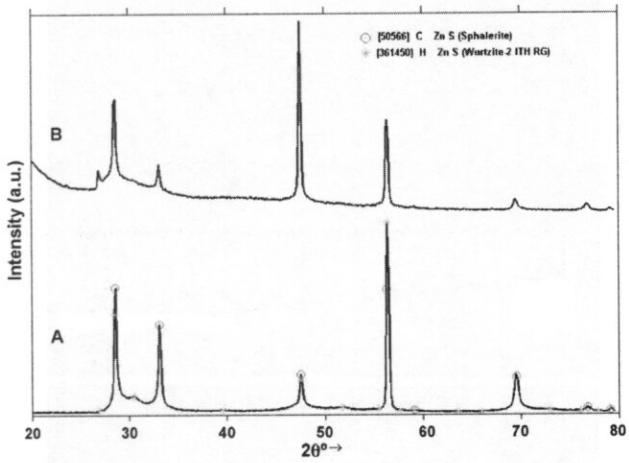

Fig. 7. XRD patterns recorded for CVD ZnS. (A) Perpendicular to direction of coating and (B) parallel to direction of coating.

marginal decrease in the density of 4.0831 g/cm^3 for CVD + HT samples and a marginal increase in density value to 4.0860 g/cm^3 for CVD + HIP samples. During HIPing process, high temperature recrystallization occurs which bring the structure of material close to equilibrium by virtue of the elimination of disordered structures due to non-equilibrium boundaries generated during CVD processing [24]. Further the residual porosity, generated due to the

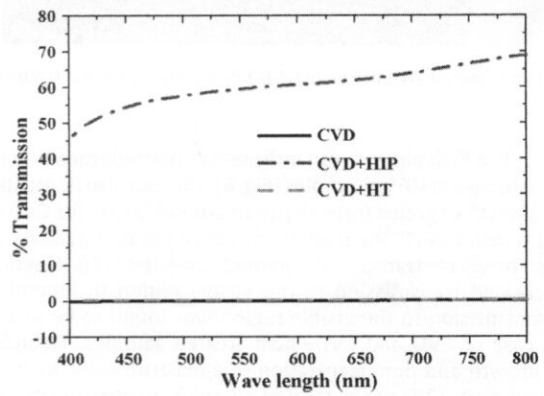

Fig. 8. Transmission patterns recorded for CVD, CVD + heat treated, CVD + HIP samples in the 400–800 nm region (CVD + HT and CVD patterns are merged at the bottom).

Table 2
Strength and hardness data of CVD ZnS samples before and after HIPing.

Properties	CVD samples	CVD + HIP samples
Knoop hardness (kg/mm^2)	210	180
Strength (three point bend) (MPa)	79	50

removal of Zn–H, was also eliminated during HIPing as evidenced by a marginal increase in density.

There have been considerable changes in the mechanical behavior of the samples on HIPing and the effects are summarized in Table 2. A decrease in the Knoop hardness from 210 kg/mm^2 (average of 5 samples) to 180 kg/mm^2 (average of 5 samples) and a decrease of bend strength from 79 to 50 MPa (average of 5 samples) was observed as a result of HIPing. This can be attributed to the increase in grain sizes from 5 to 10 μm in case of CVD samples to larger grains of ~50 μm sizes in CVD + HIP and CVD + HT samples.

4. Conclusions

Hot isostatic pressing and pressureless heat treatment in argon of ZnS samples imparted a preferred crystallographic orientation along the (1 1 1) plane as evident from the XRD transverse I ratio calculations. The removal of Zn–H absorption band most commonly observed in CVD ZnS samples can be effected by a post-CVD heat treatment at temperatures around 950 °C. However, in the absence of pressure microporosity is generated leading to the lowering of transmission values in the near IR and visible spectral regions. Simultaneous application of temperature and pressure during HIPing results in a uniform transmission >70% in the near IR regime and around 68% in the visible (400–700 nm) region.

References

[1] R. Sharma, B.P. Chandra, D.P. Bisen, Chalcogenide Lett. 6 (2009) 251.
[2] S. Senthil Kumar, R. Thamiz Selvi, Appl. Phys. A: Mater. Sci. Proc. 94 (2009) 123.
[3] H. Wang, Z. Chen, Q. Cheng, L. Yuan, J. Alloys Compd. 478 (2009) 872.
[4] M. Bredol, J. Merikhi, J. Mater. Sci. 33 (1998) 471.
[5] R. Vacassy, S.M. Scholz, J. Dutta, H. Hoffmann, C.J.G. Plummer, G. Carrot, J. Hilborn, M. Akinc, Mater. Res. Soc. Symp. Proc. 501 (1998) 369.
[6] M. Bredol, K. Matras, A. Szatkowski, J. Sanetra, A.P. Schwab, Sol. Energy Mater. Sol. Cells 93 (2009) 662.
[7] X. Wu, K.W. Li, H. Wang, J. Alloys Compd. 487 (2009) 537.
[8] A. Ghosh, A.S. Upadhyaya, Infrared Phys. Technol. 52 (2009) 109.
[9] D.C. Harris, M. Boronowski, L. Henneman, L. LaCroix, C. Wilson, S. Kurzius, B. Burns, K. Kitagawa, J. Gembarovic, S.M. Goodrich, C. Staats, J.J. Mecholsky, Opt. Eng. 47 (2008) 114001–114011.
[10] D.C. Harris, in: B.F. Andresen, M.S. Scholl (Eds.), Proceedings of SPIE Infrared Technology XXI, vol. 2552, 1995, p. 325.
[11] R. Sahraei, G.M. Aval, A. Goudarzi, J. Alloys Compd. 466 (2008) 488.
[12] M. Ladar, E.-J. Popovici, I. Baldea, R. Grecu, E. Indrea, J. Alloys Compd. 434–435 (2007) 697.
[13] V.I. Gayou, B.S. Hernandez, M.E. Constantino, E.R. Andres, T. Diaz, R.D. Macuil, M.R. Lopez, Vacuum, doi:10.1016/j.vacuum2009.10.023.
[14] Z.Z. Zhang, D.Z. Shen, J.Y. Zhang, C.X. Shan, Y.M. Lu, Y.C. Liu, B.H. Li, D.X. Zhao, B. Yao, X.W. Fan, Thin Solid Films 513 (2006) 114.
[15] P.P. Hankare, P.A. Chate, D.J. Sathe, A.A. Patil, Appl. Surf. Sci. 256 (2009) 81.
[16] J.S. Goela, R.L. Taylor, J. Mater. Sci. 23 (1988) 4331.
[17] J.H. Park, T.S. Sudarshan (Eds.), Surface Engineering Series, vol. 2, ASM International, Materials Park, OH, 2001.
[18] R.L. Gentilman, B.A. Dibenedetoo, R.W. Tustison, J. Pappis, in: O. Hugh, Person (Eds.), Chemically Vapour Deposited Coatings, The American Ceramic Society Inc., Ohio, 1981, p. 46.
[19] J.A. Savage, Glass Technol. 32 (1991) 35.
[20] Y. Drezner, S. Berger, M. Hefetz, Mater. Sci. Eng. B87 (2001) 59.
[21] G.J. Reddy, E.S.B. Rao, Int. J. Powder Metall. 31 (1995) 265.
[22] J. Zhang, A.J. Ardell, J. Mater. Res. 6 (1991) 1950.
[23] F. Zhenyi, C. Yichao, H. Yongliang, Y. Yaoyuan, D. Yanping, Y. Zewu, T. Hongchang, X. Hongtao, W. Heming, J. Cryst. Growth 237–239 (2002) 1707.
[24] E.V. Yashina, E.M. Gavrishchuk, V.B. Ikonnikov, Inorg. Mater. 40 (2004) 901.
[25] A.F. Shchurov, E.M. Gavrishchuk, V.B. Ikonnikov, E.V. Yashina, A.N. Sysoev, D.N. Shevarenkov, Inorg. Mater. 9 (2004) 336.

Please cite this article in press as: P. Biswas, et al., J. Alloys Compd. (2010), doi:10.1016/j.jallcom.2010.01.120

[26] A.F. Shchurov, V.A. Perevoshchikov, T.A. Gracheva, N.D. Malygin, D.N. Shevarenkov, E.M. Gavrishchuk, V.B. Ikonnikov, E.V. Yashina, Inorg. Mater. 9 (2004) 96.
[27] S. Suzuki, S. Kitagawa, H. Iwata, Y. Sasaki, J. Cryst. Growth 134 (1993) 67.
[28] T. Bansagi, E.A. Secco, O.K. Srivastava, R.R. Martin, Can. J. Chem. 46 (1968) 2881.
[29] L.A. Xue, R. Raj, J. Am. Ceram. Soc. 72 (1989) 1792.
[30] S.S. Singh, S. Pratap, J. Prasad, R. Kumar, K. Murari, Ind. J. Eng. Mater. Sci. 8 (2001) 18.
[31] J.S. Goela, J. Askinazi, B. Robinson, Proceedings of SPIE, vol. 4375, 2001, p. 114.
[32] C.S. Chang, J.L. He, Z.P. Lin, Wear 255 (2003) 115.
[33] V.K. Wadhawan, S.M. Gupta, S.K. Pathak, M.K. Jain, K. Muralidhar, V. Eswaran, Proceedings of the International School on Crystal Growth of Technological Important Electronic Material, 2003, p. 523.

Please cite this article in press as: P. Biswas, et al., J. Alloys Compd. (2010), doi:10.1016/j.jallcom.2010.01.120